

# Potential *in vitro* and *ex vivo* targeting of bZIP53 involved in stress response and seed maturation in *Arabidopsis thaliana* by five designed peptide inhibitors

Prateek Jain<sup>a,b</sup>, Koushik Shah<sup>a,b</sup>, Vikas Rishi<sup>a,\*</sup>

<sup>a</sup> National Agri-Food Biotechnology Institute, Knowledge City, Sector 81, Mohali, Punjab 140306, India

<sup>b</sup> Department of Biotechnology, Panjab University, Chandigarh, Punjab 160014, India

## ARTICLE INFO

### Keywords:

bZIP proteins  
Coiled coil  
Peptide inhibitor  
Protein-protein interactions  
DNA-binding  
Dimerization

## ABSTRACT

Basic leucine zipper (bZIP) transcription factors (TFs) are eukaryote-specific proteins that bind to DNA as a homodimer or heterodimer and regulate gene expression. They are involved in several biological processes in plants; therefore inhibiting bZIP-DNA binding activity by targeting protein-protein interface is an attractive proposition with aspects of both basic and applied biology. Here, we describe the equilibrium and kinetic interactions studies of a designed peptide inhibitor A-ZIP53 and its four variants with the bZIP53 protein, a key regulator of seed maturation phase and stress response in *Arabidopsis*. Five designed peptide inhibitors were primed to preferentially interact with bZIP53 and inhibit its DNA binding activity. Isothermal circular dichroism (CD) studies were used to quantify the structural changes accompanying heterodimers formation between bZIP53 and five A-ZIP53s. Equilibrium studies using electrophoretic mobility shift assay (EMSA) and fluorescence polarization (FP) assays suggest that A-ZIP53s and bZIP53 mixture form heterodimers, incapable of binding to DNA. Four A-ZIP53 derivatives were designed with additional interactions that drive heterodimerization with bZIP53. A-ZIP53s dose-dependent FP studies show that peptide inhibitors displaced the DNA bound bZIP53 with nM half-maximal inhibitory (IC<sub>50</sub>) concentrations. Using FP, time-dependent displacement kinetic studies were used to rank five A-ZIP53s for their abilities to displace DNA-bound bZIP53 with a rank order of A-ZIP53 < A-ZIP53(A → E) < A-ZIP53(N → A) < A-ZIP53(R → E) < A-ZIP53(A → E, N → A). In transient transfection assays, bZIP53-mediated GUS activity was inhibited by equimolar concentrations of five A-ZIP53s with A-ZIP53(A → E, N → A) the most effective one. Similar peptide inhibitors may be designed against other bZIP proteins to study their functions *in vivo*.

## 1. Introduction

Basic leucine zipper (bZIP) transcription factors (TFs) are exclusively eukaryotic class of dimeric proteins that regulate a broad range of biological processes, either as homodimers or heterodimers [1–4]. A bZIP TF has an N-terminal DNA binding domain and a C-terminal coiled coil dimerization domain which is characterized by the repeat of seven amino acids or a heptad designated as (gabcdef)<sub>n</sub> [5]. In *Arabidopsis*, bZIP TFs are involved in pathogen defense, light signaling, flower development, seed development and maturation [6–8]. The phenomenon of seed maturation is under the control of the combinatorial action of the multiple bZIP TFs including bZIP53, bZIP10, and bZIP25. The involvement of the bZIP53 TF has further been reported in salt and starvation-mediated stress response [9,10]. Thus, bZIP53 implication in different signaling and metabolic pathways makes it an

important and pertinent molecular target to inhibit.

Targeting bZIP TFs is rewarding but challenging as they lack the enzymatic pocket, have wider range of topographies and large surface area at the DNA binding and protein-protein interfaces [11,12]. Given the significance of the bZIPs in various biological processes, it is important to use the molecules that selectively disrupt the dimer formation or the bZIP-DNA interactions [13–15]. The availability of the high-throughput screening (HTS), computer-aided molecular docking and other approaches have contributed in the designing of small molecules that may work as an inhibitor of the bZIP-DNA complex or affect the bZIP dimerization. [16–18]. Currently, various classes of inhibitory molecules are available, including small molecules, polyamides, and effector domains but their efficacy and specificity in disrupting the bZIP dimerization or bZIP-DNA interactions are debatable [19–21]. Earlier attempt to inhibit bZIPs with small molecules have met with limited

\* Corresponding author.

E-mail address: [vikasrishi@nabi.res.in](mailto:vikasrishi@nabi.res.in) (V. Rishi).

<https://doi.org/10.1016/j.bbapap.2018.09.007>

Received 27 March 2018; Received in revised form 31 August 2018; Accepted 25 September 2018

Available online 29 September 2018

1570-9639/ © 2018 Elsevier B.V. All rights reserved.

success, while use of other regulatory biological tools like the RNAi and CRISPR/cas9 are restricted by their off-target effects [1,18,19,21–24]. In nature, truncated isoforms or dominant negative forms of transcription factors are often used for modulating the gene activity. For example, C/EBP $\beta$  LIP, a dominant negative isoform lacking transactivation domain inhibits the activity of biological active C/EBP $\beta$  LAP isoform by forming a heterodimer [25]. Similarly, in plants, truncated transcription factor-like proteins called microProteins (miPs) are known to modulate transcription factor activities [26]. Designed peptides or peptidomimetics have major advantages over small molecules and naturally occurring dominant negative forms of TFs as they mimic natural dimerizing partners and can be designed to interact with high affinity and specificity to the target proteins [1]. Previously, several peptide inhibitors have been reported that disrupts the protein-protein interface of bZIP's dimerization domain and few are in clinical trials [27–29].

Earlier, we have designed dominant negative peptide inhibitor A-ZIP53 that prevented bZIP53 binding to a G-box containing DNA. We used this peptide to elucidate the structural determinants that drive the heterodimerization between bZIP53, bZIP10, and bZIP25. A-ZIP53 was designed by replacing the basic DNA binding domain of bZIP53 with the rationally designed 28 amino acids long peptide, rich in glutamic acid. Further four peptides were designed with additional interactions that drive heterodimerization. Equilibrium studies, using CD and mass spectrometry showed strong interactions between bZIP53 and A-ZIP53 and its four derivatives but the study did not envisage whether A-ZIP53 can displace bZIP53 from DNA-bZIP53 complex *in vitro*, a property that is prerequisite to its biological activity [30]. Here we further attempt to answer if heterodimerization between bZIP53 and A-ZIP53 takes place in biological relevant temperature and timescale. Building on our previous work, now we have performed kinetics of displacement of bZIP53 bound to a G-box DNA by five A-ZIP53s. FP was used to measure binding affinity of bZIP53 and A-ZIP53 and IC<sub>50</sub> values were determined for five A-ZIP53 peptide inhibitors. Quantitative structural changes accompanying heterodimer formation between bZIP53 and five A-ZIP53s are provided by equilibrium CD studies. Using *Arabidopsis* protoplasts, *ex vivo* transient transfections studies demonstrated the efficacies of five A-ZIPs in inhibiting the bZIP53-mediated GUS reporter activities.

## 2. Materials and methods

### 2.1. Plasmid vectors

Plasmid vectors containing full-length and DNA binding domain ORFs of bZIP53, five A-ZIP53s and A-ZIP39 are described previously. All proteins used in the present study have T7 epitope (ASMTGGQ-QMG) at their N-terminal. bZIP53 and A-ZIP53 nucleotide sequences were confirmed by dideoxy sequencing. The amino acids sequence of bZIP53 is as follow: RYATVTDERKRKRMSNRESARRSRMRKQQLGDLINVEVTLKNDNAKITEQVDEASKKYIEMESKNNVLRQASELTDRLRSLNSVLEMVVEISGQALD.

All five designed protein inhibitors have the same c-terminal dimerization domain. The acidic extensions of five A-ZIP53s with underlined mutated amino acids and sequence of A-ZIP39 are as follow:

A-ZIP53: LEQRAEELARENEEKEAEELEQELAELEN—  
 A-ZIP53(A → E): LEQRAEELERENEKEAEELEQELAELEN—  
 A-ZIP53(R → E): LEQEAELARENEEKEAEELEQELAELEN—  
 A-ZIP53(N → A): LEQRAEELAREAELEKEAEELEQELAELEN—  
 A-ZIP53(A → E, N → A): LEQRAEELEREAEELEKEAEELEQELAELEN—  
 A-ZIP39: LEQRAEELARENEEKEAEELEQELAELENELNQLKEENAQLKHALAELEKRRKQYFESLKSRAQPKLPKSNGLRLTLMRNPSCPL.  
 bZIP39 expression vector was a gift from Dr. Wolfgang DrÖge-Laser, University of Würzburg, Germany.

### 2.2. Expression and purification of proteins

All chemicals used in the study were of highest analytical grade. Plasmids encoding bZIP53, bZIP39, A-ZIP53s and A-ZIP39 were used for the transformation of *E. coli* BL21 (DE-3). Transformed cells were grown overnight at 37 °C, and 300 rpm in 20 ml Superbroth medium containing 100  $\mu$ g/ml ampicillin and 35  $\mu$ g/ml chloramphenicol. High-density cultures were transferred to the 500 ml Superbroth medium containing 100  $\mu$ g/ml ampicillin. Transformed bacteria were grown at the 37 °C, and 300 rpm until the O.D. reached 0.6. Bacterial cultures were induced by the addition of 1 mM isopropyl- $\beta$ -D-thiogalactopyranoside (IPTG) and harvested after 3–5 h of growth and processed as described earlier [31]. Samples were dialyzed overnight against the low salt buffer (20 mM Tris-HCl (pH 8.0), 50 mM KCl, 1 mM EDTA, 0.2 mM phenylmethylsulfonyl fluoride (PMSF), and 1 mM DTT). The bZIP53 and bZIP39 proteins were purified over the heparin-sepharose column and eluted using potassium phosphate buffer (pH 7.4) containing increasing concentrations of the KCl (150, 300, and 1000 mM). A-ZIP53 proteins were purified using hydroxyapatite column and eluted with the 250 mM sodium phosphate buffer (pH 7.4). All proteins were subsequently purified using reverse phase HPLC as described previously [31]. 300 mM and 1 M fractions of bZIP proteins and 250 mM Na-phosphate fraction of A-ZIP proteins were injected into C18 Reverse Phase column (Agilent, USA). Gradient of solution A (degassed deionized water with 0.1% TFA) and solvent B (100% acetonitrile with 0.1% TFA) was employed for protein purification. Gradient of 0–100% of solvent B with a flow rate of 2 ml/min was used to elute proteins from the column. Real time elution was monitored by taking absorption at 220 nm. Complete elution was achieved in 45 mins. Purified lyophilized proteins were dissolved in the CD buffer (12.5 mM phosphate buffer (pH 7.4), 150 mM KCl, and 0.25 mM EDTA) and concentrations were measured by using absorption values at 230 nm [31].

### 2.3. Protein sequencing by mass spectrometry

Amino acids sequences of expressed A-ZIP53 and its four derivatives with single and double mutations were confirmed by Nano-LC-MS/MS. Protein sequencing was performed on Triple TOF<sup>M</sup> 5600 mass spectrometer (AB Sciex Pte. Ltd., USA) attached to the Nano-LC (Eksigent Technologies Llc, USA). For peptide sequencing, lyophilized tryptic digests of 0.1  $\mu$ g protein were re-suspended in 0.1% formic acid [32]. 10  $\mu$ l of sample was passed through desalting trap column (Chrom-XP, C-18-CL-3  $\mu$ M, 350  $\mu$ M  $\times$  0.5 mm, Eksigent Technologies LLC., USA). Peptides were separated on the C<sub>18</sub> matrix column (3C-18-CL-120, 3  $\mu$ M, 120A, 0.075  $\times$  150 mm, Eksigent Technologies LLC., USA). The analyte was eluted using gradient of mobile phase A (MS grade water with 0.1% formic acid) and mobile phase B (acetonitrile with 0.1% formic acid) from 5 to 95% B in 32 min with a flow rate of 300 nl/min. After separation, peptides were subjected to tandem mass (MS/MS) analysis. Peptides were identified using Protein Pilot software (Version 4.08085, AB Sciex Pte. Ltd., USA).

### 2.4. FP assays

For FP, 5' fluorescein labeled 28-mer double-stranded oligo containing a single G-box binding site for bZIP53 protein (GTCAGTCAGG CCACGTGGCATGCCTCAG) was used as described earlier [30]. Same oligo was used for studies involving bZIP39. Previously, FP was used to study DNA-protein interactions [18]. 5 nM probe was added to 96 well black polypropylene microwell plate (Thermo Fischer Scientific, USA) in the FP buffer (10 mM Tris pH 7.4, 150 mM KCl, 0.5 mM EDTA, 0.1% Triton X-100, and 0.2 mM DTT). Double-stranded oligo in FP buffer was equilibrated for 30 min at 25 °C and FP signals were recorded using SpectraMax M5<sup>e</sup> (Molecular Devices, USA) with excitation at 485 nm and emission at 535 nm with high sensitivity setting. To study dose-dependent changes in FP signals, varying concentrations of bZIP53

protein (10, 50, 250, 500, and 1000 nM) were subsequently added to oligo containing polypropylene plate, the mixtures were incubated for 1 h at 25 °C and fluorescence signals were recorded. Increased fluorescence signals represented bZIP53-DNA binding. For probing the efficiency of peptide inhibitor A-ZIP53 and its derivatives against bZIP53-DNA binding, two sets of experiments were performed. In first equilibrium experiments *i.e.*, scheme 1, prior to adding DNA, 500 nM of bZIP53 protein was heated to 65 °C, in presence of 1 μM A-ZIP53 peptide inhibitor, incubated for 15 mins and then added to fluorescein-labeled DNA. Mixtures were incubated at 25 °C for 2 h in dark. Lower FP signals observed were due to the inability of A-ZIP53|bZIP53 heterodimer to bind DNA. In second set of experiments or scheme 2, bZIP53 was allowed to bind to labeled DNA, incubated at 25 °C for 1 h for DNA-bZIP53 complex to form. DNA binding of bZIP53 was challenged by adding increasing concentrations of five A-ZIP proteins. Solutions containing DNA-bZIP53 complex and different A-ZIPs were incubated for 1 h at 25 °C and polarization signals were measured again. A-ZIP39 that does not heterodimerize with bZIP53 was used as negative control [30]. For displacement kinetic assays 1 μM of five A-ZIP53s were added to DNA-bZIP53 complex and polarization signals were immediately and continuously recorded over 1 h. B-ZIP39, a non-target of A-ZIP53 was used as a negative control [30].

## 2.5. Protein structure modelling

bZIP53 homodimer, DNA-bound bZIP53 dimer, A-ZIP53 homodimer and the A-ZIP53|bZIP53 heterodimer (vertical line indicates heterodimer) were modeled using SWISS-MODEL [33,34]. PyMol software was used for molecular visualization of protein [35]. For the modelling of bZIP53, *Arabidopsis* HY5 bZIP was used as a template. DNA-bound bZIP53 was modeled on C/EBPα homodimer, whereas NF-κB essential modulator was the template for A-ZIP53(A → E). Heterodimer between A-ZIP53(A → E) and bZIP53 used cfos and Jun heterodimer as template. Here, we emphasized that models are for visualization only.

## 2.6. CD spectroscopy

CD studies were carried out using J815 spectropolarimeter (Jasco, Japan) with a 5 mm rectangular CD cell. All protein samples were dissolved in the standard CD buffer (12.5 mM potassium phosphate (pH 7.4), 150 mM KCl, and 0.25 mM EDTA). For CD study, protein samples were heated at 65 °C for 15 min with 1 mM DTT, cooled at room temperature and diluted to 2 μM dimer in 1 ml buffer. Wavelength scans in triplicate were performed at 6 °C from 200 to 260 nm. Far-UV spectra were measured with 50 nm/min scanning speed, 1 min response time, and 3 accumulations. The Spectra Manager program (Jasco Corp.) was used for buffer subtraction. All CD spectra were represented as the mean-residual weight molar ellipticity,  $[\theta]_{MRW}$ , in deg.cm<sup>2</sup>/dmol.

$$[\theta]_{MRW} = \frac{100 \times \theta}{C \times N \times l} \quad (1)$$

where  $\theta$  is ellipticity signal in deg., C is the molar protein concentration, N is the number of amino acids and l is the path length of CD cuvette.

## 2.7. EMSA assays

A 28 bps fluorescein labeled DNA that was employed in FP was used as probe for EMSA assays. EMSA assays involving bZIP53 and A-ZIP53s heterodimers, proteins were incubated in the gel shift reaction buffer (10 mM Tris (pH 8.0), 150 mM KCl, 0.5 mM EDTA, 0.3% glycerol, 0.1% BSA, and 0.1% Triton-X 100) heated to 65 °C for 10 mins, cooled to room temperature and mixed with the fluorescein labeled double-stranded oligos. Reaction mixtures were incubated in dark at room temperature for 2 h and were resolved using 5% native PAGE [30]. Gels

were visualized in UVP gel documentation system with excitation at 485 nm and emission at 535 nm.

## 2.8. Transient transfections

Transient transfections were performed in *Arabidopsis thaliana* protoplast system. Detail method for protoplast isolation is described elsewhere [6,30,36]. 10<sup>6</sup>–10<sup>7</sup> protoplasts were isolated using 40–50 leaves. Leaf sections were cut and lysed using 10 ml of enzyme solution (20 mM MES (pH 5.7), 1.5% cellulase, 0.4% macerozyme (Sigma, USA), 0.4 M mannitol, and 20 mM KCl) at 37 °C with gentle shaking at 90 rpm in dark. Leaf tissues endogenous DNAs and proteases were inactivated by heating the solution to 55 °C for 10 mins. Solution with leaf sections was cooled to room temperature, and 10 mM CaCl<sub>2</sub>, 3 mM β-mercaptoethanol, and 0.1% BSA were added. Leaf sections were vacuum infiltrated in desiccator for 30 min in dark. Sections were further incubated in dark for 3–4 h with gentle shaking. Lysis was considered complete when the solution turned green. Intact protoplasts were checked under the microscope. Protoplasts were diluted by adding appropriate volume of W5 buffer (2 mM MES (pH 5.7), 154 mM NaCl, 125 mM CaCl<sub>2</sub>, and 5 mM KCl). Debris was removed by filtration and protoplasts were centrifuged at 100g, re-suspended at a density of 2 × 10<sup>5</sup>/ml in W5 buffer.

For transfections, GUS was used as reporter plasmid whereas NAN coding plasmid was used as an internal control. 3 μg each of reporter plasmids *i.e.*, CaMV35S:GUS and CaMV35S:NAN, equal molar ratio of the effector plasmids; CaMV35S:bZIP53, and A-ZIPs encoding plasmids, namely, CaMV35S:A-ZIP53, CaMV35S:A-ZIP53 (A → E), CaMV35S:A-ZIP53 (N → A), CaMV35S:A-ZIP53 (R → E), double mutant CaMV35S:A-ZIP53 (A → E, N → A) and CaMV35S:A-ZIP39 were used as reported earlier [6,30]. Protoplasts were transfected using PEG (20% PEG 3500 in 200 mM mannitol and 100 mM CaCl<sub>2</sub>). Protoplasts were re-suspended in 1 ml W1 solution (4 mM MES (pH 5.7) 0.5 M mannitol, and 20 mM NaCl) and incubated at 25 °C for 16–18 h in dark. Reporter gene activity was checked using GUS/NAN reporter assay as described previously [6,36]. A-ZIP39 was used as a negative control.

## 3. Results

Amino acids sequences of A-ZIP53 and four versions with single and double substitutions were confirmed by the mass spectrometry. HPLC purified, trypsin digested proteins were resolved using Nano-LC. Triple-TOF tandem MS/MS instrument was used to generate MS/MS peptide profile. For A-ZIP53s, 84–487 peptides were obtained for each protein and *Arabidopsis* protein data-base was used for peptide identification (Supplementary Table 1). Peptides were aligned for generating full amino acids sequences of proteins. Mutations were identified using Protein-pilot software.

### 3.1. Structural determinants of heterodimers formation between bZIP53 and A-ZIP53 and its four derivatives

bZIP protein has two structurally distinct domains, an unstructured N-terminal basic amino acids rich DNA-binding domain and a C-terminal leucine zipper region that spontaneously forms a dimeric coiled coil in solution. Earlier, we used five A-ZIP53s peptides, designed to interact with bZIP53 to understand the mechanistic basis of heterodimerization between bZIP53, bZIP10 and bZIP25, three bZIPs that are involved in *Arabidopsis*'s seed maturation phase but due to the low sensitivity of EMSA assays, we were not able quantify the bZIPs-DNA interactions. The present study is an attempt to quantify the interaction between bZIP53 and five A-ZIP53s, and evaluate if five heterodimers, based on their dissociation constant values, are more stable than bZIP53-DNA complex. We further set out to explore if five possible heterodimers are formed in biological relevant temperature and time-scale.

A coiled coil contains number of heptads designated by amino acids at **a**, **b**, **c**, **d**, **e**, **f** and **g** positions. Dimerizing leucine zipper is so-named due to the presence of leucine at **d** positions of heptads. Though leucine is the most conserved amino acid, bZIP53 has isoleucine, alanine, methionine and valine in **d** position of second, fourth and eighth heptad. These along with amino acids at **a** position form the hydrophobic core of the coiled coil. Additional stability is imparted by the **g** → **a'** interactions [37]. Dimerization specificity is governed by amino acids at **g** and **e'** positions and polar amino acids at **a** positions of the heptads. Due to the presence of a helix breaker proline, two consecutive glycines, and charged amino acids at **g** and **e** positions, bZIP53 leucine zipper domain is predicted to be more than eight heptads long with four attractive (1<sup>st</sup> and 4<sup>th</sup> heptads) and two repulsive (5<sup>th</sup> heptad) **g** ↔ **e'** interactions in a homodimer conformation [30]. Keeping the dimerizing leucine zipper region intact, A-ZIP53 was produced by replacing the basic DNA binding domain of bZIP53 with 28 amino acids long (equivalent to four heptads) glutamic acid rich acidic peptide. Furthermore, the acidic peptide is designed to be amphipathic in nature and is predicted to forms coiled coil with the unstructured DNA binding domain of bZIP53 [38]. In an equimolar mix, A-ZIP53 heterodimerizes with bZIP53 and the complex is inept in DNA binding, resulting in downregulation of bZIP53-mediated gene expression [30]. Supplementary Fig. 1 shows the coiled coil representation of A-ZIP53|bZIP53 heterodimer.

To be an effective peptide inhibitor, A-ZIP53 dimer must unfold into monomers and heterodimerize with the target wild-type bZIP TF. Four additional derivatives of A-ZIP53 namely, A-ZIP53(A → E), A-ZIP53(N → A), A-ZIP53(R → E), and A-ZIP53(A → E, N → A) were designed with decreasing homodimer stability and increasing heterodimer stabilities with bZIP53 [30]. A-ZIP53(A → E) has a glutamic acid that replaced alanine at the **e** position of 1<sup>st</sup> heptad of acidic extension resulting in an additional salt bridge (**K** ↔ **E**) in the A-ZIP53(A → E)|bZIP53 heterodimer. Similarly, substitution of R → E in the 1<sup>st</sup> heptad of A-ZIP53 introduced a stable **g** ↔ **a'** interaction in A-ZIP53(R → E)|bZIP53 complex. In A-ZIP53(N → A) peptide, asparagine at **a** position of 2<sup>nd</sup> heptad (L<sub>-2</sub>) strongly favors homodimerization, substitution with an alanine decreased its homodimer stability and promote heterodimer formation with bZIP53 [39,40]. A double-substituted A-ZIP53 peptide inhibitor (A → E, N → A) showed the lowest homodimer stability but has the highest heterodimer stability with bZIP53 [30]. Thermal stability studies involving bZIP53 homodimer and its heterodimers with five A-ZIP proteins were used to determine  $K_D$  values (dissociation constant) [30].  $K_D$  value for bZIP53-DNA binding was obtained by FP (this study). Fig. 2 shows the models of coiled coils of bZIP53, bZIP53 bound to DNA, A-ZIP53(A → E), and A-ZIP53|bZIP53 heterodimer. Note that the models are generated for visualization only. bZIP53-DNA complex is ~ 1.5 fold stable than bZIP53 dimer alone whereas A-ZIP53|bZIP53 heterodimers are ~ two to four magnitude more stable than bZIP53-DNA complex suggesting their possible *in vivo* functionality ( $K_D$ , A-ZIP53|bZIP53 =  $2 \times 10^{-11}$ ,  $K_D$ , A-ZIP53(A → E)|bZIP53 =  $6 \times 10^{-11}$ ,  $K_D$ , A-ZIP53(R → E)|bZIP53 =  $3 \times 10^{-11}$ ,  $K_D$ , A-ZIP53(N → A)|bZIP53 =  $3 \times 10^{-12}$ ,  $K_D$ , A-ZIP53(A → E, N → A)|bZIP53 =  $9 \times 10^{-13}$ ).

### 3.2. DNA binding of bZIP53 as probed by FP

FP was used to study the DNA binding of bZIP53. 5'-Fluorescein labeled 28 bps long double-stranded DNA with a centrally placed G-box containing 6 bps binding sequence was used to probe the DNA-binding of bZIP53. 5 nM labeled DNA was titrated with increasing concentrations of pure bZIP53 protein. Bare labeled DNA, in the absence of binding, tumbles fast and gave low fluorescence polarization signals. Binding of bZIP53 reduces the tumbling rate of DNA, resulting in increased FP signal (Supplementary Fig. 2). FP signals as the function of protein concentrations were used to measure the DNA binding affinity of bZIP53. Fig. 1A shows the change in fluorescence signals when 50, 100, 250, 500 and 1000 nM of bZIP53 protein was added to 5 nM

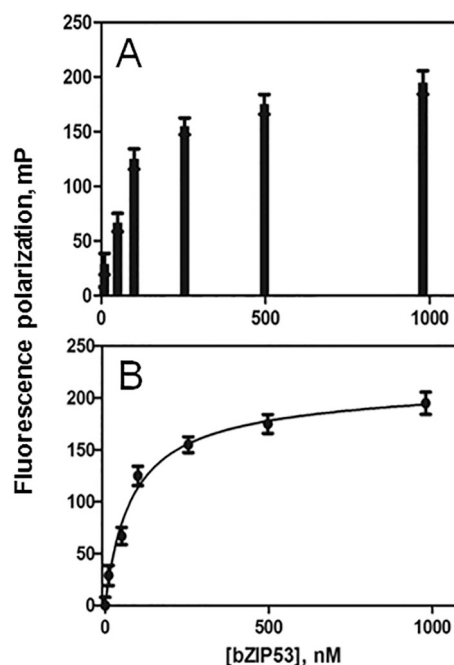


**Fig. 1.** FP assays showing the binding of bZIP53 protein to fluorescein labeled DNA. **A)** Fluorescence polarization signal of freely tumbling DNA was increased by bZIP53 binding. Reaction mixture contained 5 nM 5'-fluorescein end labeled 28 bps double stranded DNA with a centrally placed G-box binding sequence for bZIP53. Polarization signals increased with increasing concentrations of bZIP53 protein, interpreted as bZIP53 binding to the G-box sequence. Each data point is an average of six independent experiments and error bars represent SEs of the mean. **B)** Data from **A)** was used to draw binding curve for bZIP53 protein. Data points were fitted according to Eq. (2) that yielded a  $K_D$  of 37.1 nM.

fluorescein labeled G-box containing DNA in FP buffer (10 mM Tris pH 7.4, 150 mM KCl, 0.5 mM EDTA, 0.1% Triton X-100, and 0.2 mM DTT). Each mixture was incubated at 25 °C for one hour and fluorescence signals were recorded. Polarization signals were plotted for five bZIP53 concentrations. Each data point was an average of six independent experiments. Fig. 3B shows the fitting of binding curve according to Eq. (2).

$$\frac{FP_{max}}{K_D + x} \quad (2)$$

where  $FP_{max}$  is the FP signal at saturating bZIP53 concentrations.  $K_D$  is the equilibrium dissociation constant. A  $K_D$  value of 37 nM for bZIP53 binding to G-box was obtained which is in good agreement with earlier reported values for other bZIP TFs DNA-binding [41].

### 3.3. Stability of bZIP53, A-ZIP53 homodimer and five heterodimers

$K_D$  was used to define the stability of bZIP53 alone and when bound to DNA and A-ZIP53 homodimers and [30]. bZIP53 bound to DNA with a  $K_D$  of 37.1 nM.

### 3.4. CD spectroscopy studies show the structural changes accompanying heterodimers formation

CD spectroscopy was used to quantify heterotypic interaction between the bZIP53 and five A-ZIP53s. Fig. 2A–E shows the circular dichroic spectra from 200 to 260 nm of the bZIP53 (2 μM dimer) with the A-ZIP53 (2 μM dimer) and its derivatives (A → E, R → E, N → A and a double substitution (A → E, N → A)). The raw signals in milli degree ellipticity (θ, mdeg) were converted into concentration independent mean-residual weight molar ellipticity values  $[\theta]_{MRW}$ . The far-UV CD spectrum of all proteins and their heterodimers show minima at 222

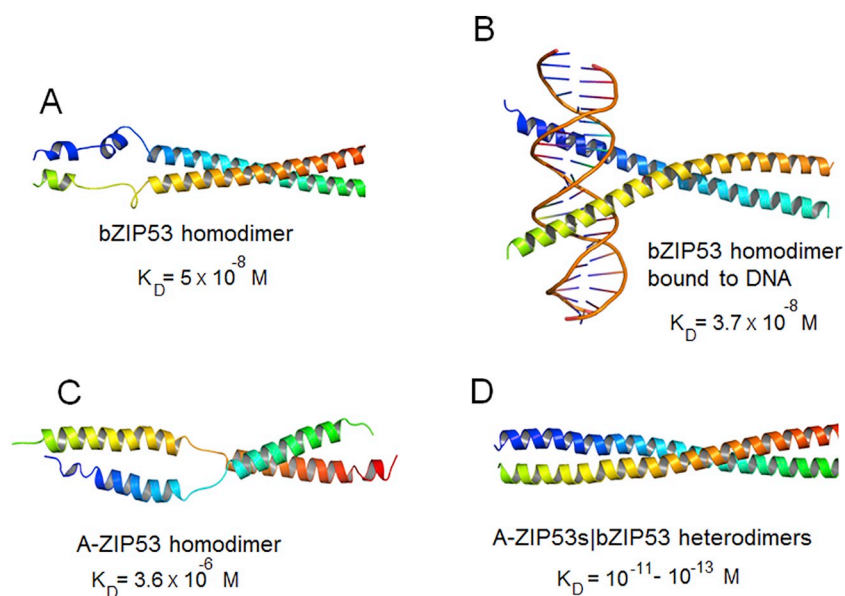


**Fig. 2.** Structural models of bZIP53 alone, DNA bound bZIP53, and A-ZIP53|bZIP53 heterodimer. Note that models are for visualization only. Based on  $K_D$  values, in equilibrium conditions, A-ZIP53|bZIP53 heterodimer is the preferred conformation. **A)** Coiled coil model of bZIP53 dimer. N-terminus lacks structure due to repulsion in the basic DNA binding domain of the protein. A  $K_D$  of  $5 \times 10^{-8} \text{ M}$  was obtained from thermal stability studies [30]. **B)** Coiled coil is extended to N-terminus once bZIP53 binds to its cognate DNA sequence. Compared to bZIP53 homodimer, the structure is stabilized by  $\sim 1.5$  fold with a  $K_D$  of  $37.1 \times 10^{-8} \text{ M}$  (this study). **C)** A-ZIP53(A  $\rightarrow$  E) dimer where N-terminus is predicted to form  $\alpha$ -helices but due to repulsion in acidic extensions, coiled coil is unstable. **D)** A-ZIP53|bZIP53 heterodimers showed high stability and  $K_D$  values of five heterodimers ranged from  $10^{-11}$  to  $10^{-13} \text{ M}$  [30].

and 208 nm, characteristic of  $\alpha$ -helix and  $\alpha$ -helix interactions in a coiled coil [42]. For heterodimeric samples,  $2 \mu\text{M}$  each of bZIP53 and five A-ZIP53s were taken, thus each mixture contained  $4 \mu\text{M}$  total protein. Mixtures were heated to  $65^\circ\text{C}$  for 15 min and cooled to room temperature and incubated for 2 h. All A-ZIP53 peptides are unstable at  $25^\circ\text{C}$  [30], therefore spectra were taken at  $6^\circ\text{C}$ , and each spectrum is an average of five spectra. bZIP proteins are predominantly  $\alpha$ -helices [43].  $\alpha$ -helical content for each sample was determined from mean-residue weight molar ellipticity values using following equation [42]

$$\% \text{Helix} = \frac{[\theta]_{\text{obs}} \times 100}{39500 \times \left(1 - \frac{2.57}{l}\right)} \quad (3)$$

where  $[\theta]_{\text{obs}}$  is the mean-residue ellipticity at 222 nm, 39,500 ( $\text{deg} \cdot \text{cm}^2 / \text{dmol}$ ) is the ellipticity of a peptide of infinite length with a 100% helix,  $l$  is the peptide length. %  $\alpha$ -Helical contents for each sample thus obtained are given in Table 1. Fig. 3A shows wavelength scans of A-ZIP53, bZIP53 and their equimolar mix. bZIP53 with DNA binding domain and eight heptad long leucine zipper show a typical circular dichroic spectra with  $\alpha$ -helical content of 47%, whereas A-ZIP53 with acidic extension showed 31%  $\alpha$ -helices. Spectrum of mix of  $2 \mu\text{M}$  each of bZIP53 and A-ZIP53 showed an increase in  $\alpha$ -helical contents to 57%, this additional structure is interpreted as interaction between bZIP53 basic DNA domain and acidic extension of A-ZIP53. Also shown is the theoretical sum line obtained, if bZIP53 and A-ZIP53 do not interact. The sum line falls in between A-ZIP53s and bZIP53 and represents an average of  $[\theta]$  values of two proteins. Similar results were obtained with bZIP53 and its interaction with A-ZIP53(A  $\rightarrow$  E) (Fig. 2B),

A-ZIP53(R  $\rightarrow$  E) (Fig. 2C), A-ZIP53(N  $\rightarrow$  A) (Fig. 2D), A-ZIP53(A  $\rightarrow$  E, N  $\rightarrow$  A) (Fig. 3E).

The ratio (222/208 nm) of the mean-residual molar ellipticity is indicative of coiled coil [43]. A value  $> 1$  is interpreted as a strong interacting coiled coil. Our design strategy envision A-ZIP53 with minimum homodimer stability but high affinity for target molecule *i.e.*, bZIP53, so that in a mix of A-ZIP and bZIP proteins, heterodimer shall always be the preferred conformation. In this direction, four mutations were introduced in A-ZIP53 namely, (A  $\rightarrow$  E), (R  $\rightarrow$  E), (N  $\rightarrow$  A), and (A  $\rightarrow$  E, N  $\rightarrow$  A). Each mutation resulted in lower homodimeric stability and decrease in coiled coil structure indicated by reduction in 222/208 nm values (Table 1). A-ZIP53 (A  $\rightarrow$  E, N  $\rightarrow$  A) with 222/208 nm value of 0.83 was the least stable coiled coil. Our circular dichroic results showed that five peptide inhibitors used here are unstable under experimental conditions but forms highly stable heterodimers with target bZIP53.

### 3.5. EMSA show five A-ZIP53s inhibit the DNA-binding of bZIP53

Equilibrium EMSA was used to examine A-ZIP53 and four derivatives for their abilities to inhibit the DNA-binding of bZIP53 to 28 bp DNA. For EMSA, labeled DNA was same as used for FP experiments. For experiments involving bZIP53 and DNA binding,  $1 \mu\text{M}$  fluorescein labeled DNA was mixed with  $5 \mu\text{M}$  HPLC purified bZIP53 protein. Mixture was incubated at  $25^\circ\text{C}$  for 1 h. The abilities of five A-ZIP53s to inhibit the bZIP53 DNA binding were tested by mixing increasing concentrations of A-ZIP53 proteins. Heterodimers of bZIP53 and five A-

**Table 1**  
Structural changes associated with interaction of bZIP53 with five designed A-ZIP53s.<sup>a</sup>

Homodimers				Heterodimers			
Proteins	222/208 nm <sup>b</sup>	% $\alpha$ -helix <sup>c</sup>	$T_m$ , $^\circ\text{C}$ <sup>d</sup>	Protein mixtures	222/208 nm <sup>b</sup>	% $\alpha$ -helix <sup>c</sup>	$T_m$ , $^\circ\text{C}$ <sup>d</sup>
bZIP53	$1.09 \pm 0.04$	$47 \pm 2$	$41.9 \pm 0.5$	–			
A-ZIP53	$1.02 \pm 0.03$	$31 \pm 2$	–	bZIP53 + A-ZIP53	$0.99 \pm 0.05$	$57 \pm 1$	$51.5 \pm 0.5$
A-ZIP53(A $\rightarrow$ E)	$1.04 \pm 0.04$	$46 \pm 3$	$25.5 \pm 0.5$	bZIP53 + A-ZIP53(A $\rightarrow$ E)	$1.04 \pm 0.03$	$58 \pm 4$	$52.3 \pm 0.3$
A-ZIP53(R $\rightarrow$ E)	$1.12 \pm 0.06$	$37 \pm 2$	–	bZIP53 + A-ZIP53(R $\rightarrow$ E)	$1.02 \pm 0.03$	$44 \pm 1$	$53.1 \pm 0.3$
A-ZIP53(N $\rightarrow$ A)	$0.94 \pm 0.02$	$21 \pm 2$	–	bZIP53 + A-ZIP53(N $\rightarrow$ A)	$1.01 \pm 0.02$	$61 \pm 3$	$53.9 \pm 0.4$
A-ZIP53(A $\rightarrow$ E, N $\rightarrow$ A)	$0.83 \pm 0.03$	$32 \pm 3$	–	bZIP53 + A-ZIP53 (A $\rightarrow$ E, N $\rightarrow$ A)	$1.04 \pm 0.04$	$47 \pm 4$	$55.7 \pm 0.3$

<sup>a</sup> All measurements were carried out at  $6^\circ\text{C}$ .

<sup>b</sup> Error in estimation of 222/208 nm,  $\pm$  represent SE of the mean ( $n = 3$ ).

<sup>c</sup> Error in estimation of  $\alpha$ -helices,  $\pm$  represent SE of the mean ( $n = 3$ ).

<sup>d</sup> Values taken from previous study [30].

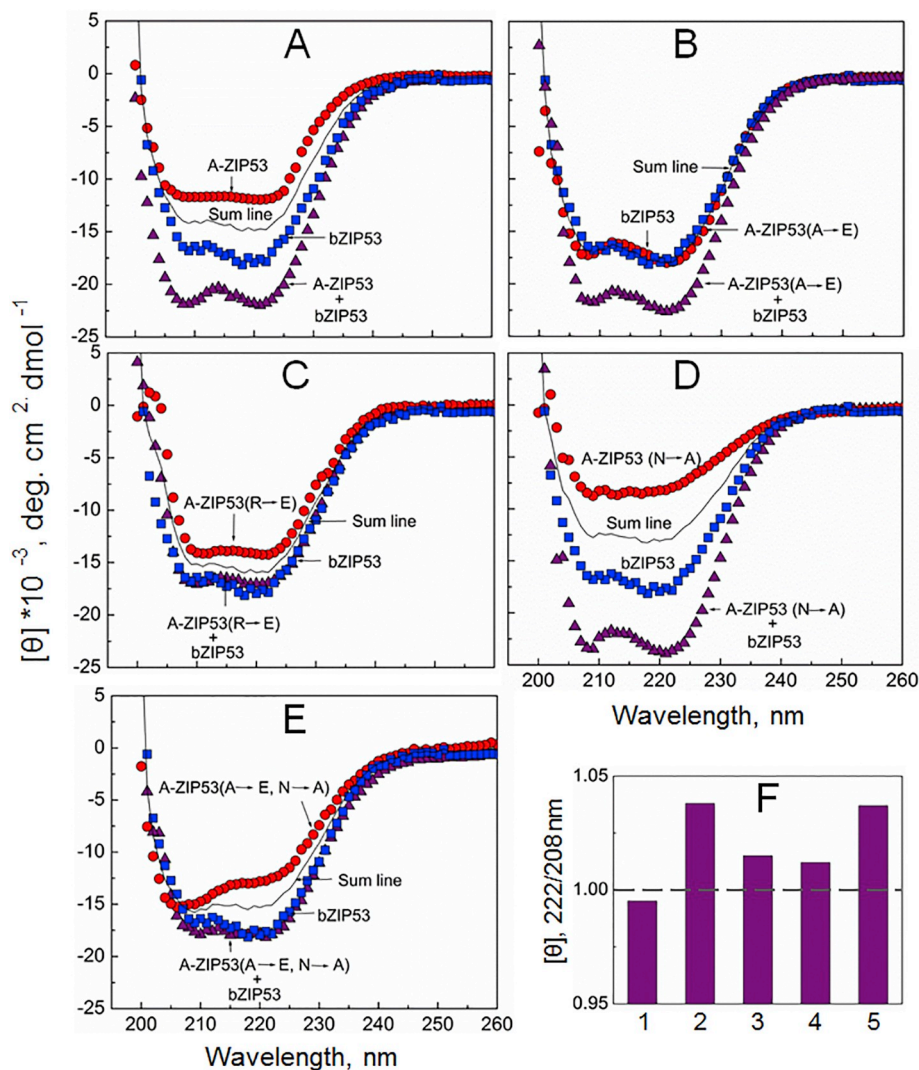


**Fig. 3.** Isothermal circular dichroic wavelength spectra from 200 to 260 nm at 6 °C of 2  $\mu\text{M}$  bZIP53, 2  $\mu\text{M}$  peptide inhibitor A-ZIP53, its four derivatives, and equimolar mix of bZIP53 and five A-ZIP53s; **A)** A-ZIP53, **B)** A-ZIP53(A  $\rightarrow$  E), **C)** A-ZIP53 (R  $\rightarrow$  E), **D)** A-ZIP53(N  $\rightarrow$  A), and **E)** A-ZIP53(A  $\rightarrow$  E, N  $\rightarrow$  A). The sum line is the assumed spectrum if the two proteins do not interact. **F)** Ratio of circular dichroic mean residual signals at 222 and 208 nm (222/208) was used to evaluate the formation of coiled coil. 222/208 nm  $\geq$  1 represents stable coiled coil.

ZIP53s were prepared by mixing 5  $\mu\text{M}$  bZIP53 with half log increasing concentrations of five A-ZIP53s (0.5, 1.5 and 5  $\mu\text{M}$ ). Mixtures were heated to 65 °C and incubated for 15 min, followed by incubation at 25 °C for 1 h and were run on 5% native PAGE. Results of five EMSA experiments are shown in Supplementary Fig. 3A–E. In all cases, DNA binding of bZIP53 is inhibited by equimolar concentrations of five A-ZIP53s.

### 3.6. FP assays demonstrate that five A-ZIP53s interact with the DNA-bound bZIP53 and inhibits its DNA binding activity

FP assays were used to evaluate the efficacies of peptide inhibitor A-ZIP53 and its derivatives in inhibiting DNA binding of bZIP53. A-ZIP53 and its derivatives are predicted to interact with the bZIP53 therefore loss in polarization signal of DNA-bZIP53 complex by peptide inhibitor is an indicator of later proficiency to form heterodimer with bZIP53. Unlike in EMSA, where prior to loading on PAGE, bZIP53 protein was mixed and heated with respective A-ZIP53, for FP assays DNA bound bZIP53 was challenged by different A-ZIP53 inhibitors. FP assays were conducted using same buffer conditions as described above. 5 nM fluorescein labeled DNA was incubated with 500 nM bZIP53 for 1 h and polarization signals were recorded (Fig. 5A–E). One hour incubation

was found to be sufficient for the reaction to reach equilibrium and further incubation has no effect on polarization signals. 1000 nM A-ZIP53 and its four derivatives were added to the DNA-bZIP53 complex, incubated for 2 h at 25 °C and polarization signals were again recorded. For each of the five experiments, FP signals decreased as five A-ZIP53s were added to DNA-bZIP53 complex, that we interpret as A-ZIPs forming heterodimers with bZIP53 (Fig. 4A–E). A-ZIPs|bZIP53 heterodimer is incapable of binding to DNA. In absence of bound bZIP53 protein, fluorescein labeled DNA tumbles fast resulting in decreased polarization signals (Supplementary Fig. 1B–C). Each data point was an average of six independent experiments.

### 3.7. FP competitive assays show $IC_{50}$ values of five A-ZIP53s

Fig. 5A–E shows the transition curves depicting changes in FP signals as the concentrations of five A-ZIP53s were increased. For dose-dependent equilibrium experiments, 500 nM bZIP53 was mixed with 5 nM fluorescein labeled G-box containing DNA. After 1 h incubation at 25 °C, 10, 50, 250, 500, 1000, and 2000 nM of A-ZIP53 and its four derivatives i.e., A-ZIP53(A  $\rightarrow$  E), A-ZIP53(N  $\rightarrow$  A), A-ZIP53(R  $\rightarrow$  E) and A-ZIP53(A  $\rightarrow$  E, N  $\rightarrow$  A) were added and mixtures were further incubated for 2 h and FP signals were recorded. Polarization signals

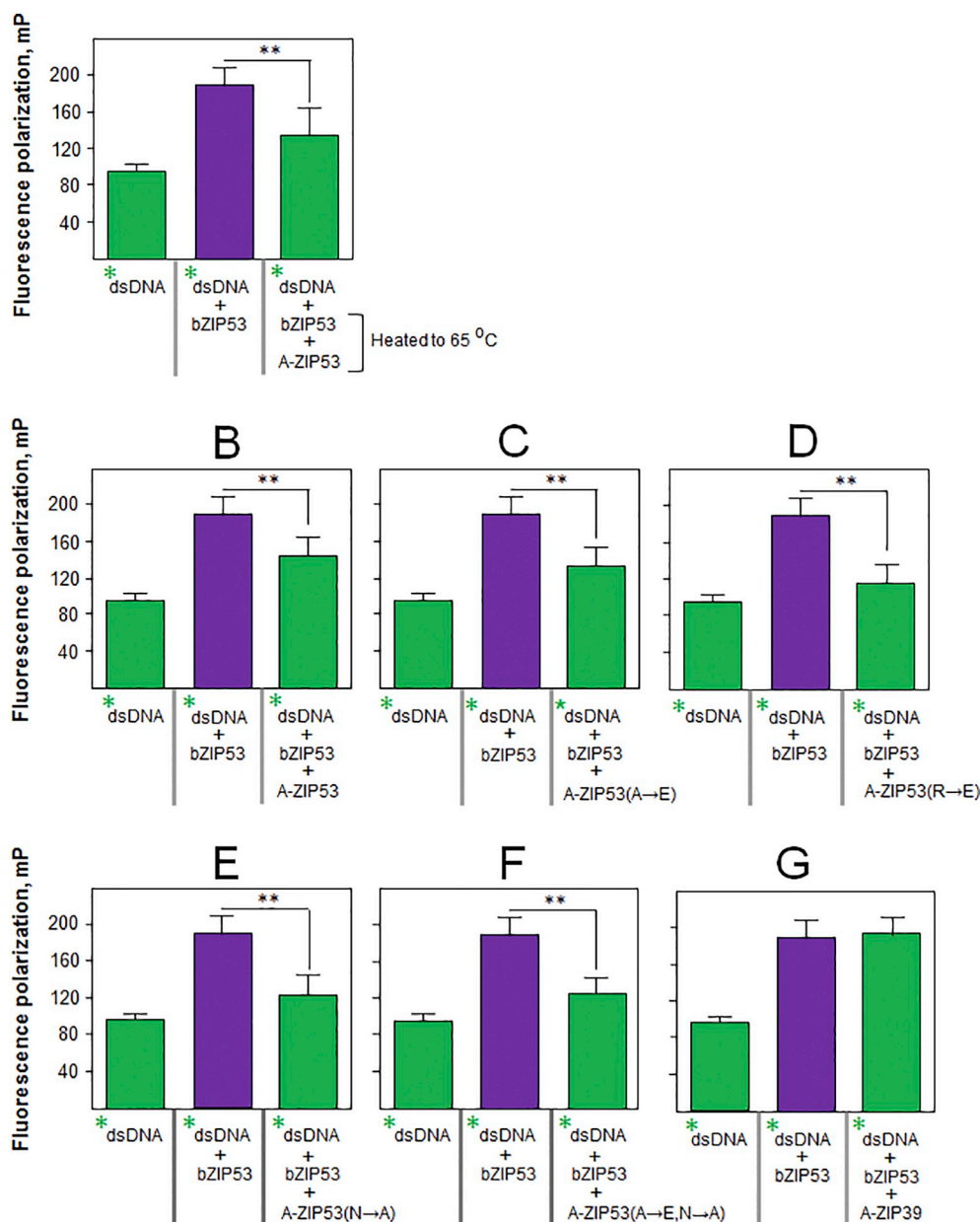


**Fig. 4.** FP assays involving two experimental schemes were used to demonstrate the impairment of DNA-bZIP53 complex by five A-ZIP53s. Green asterisks represent fluorescein labeled DNA. **A)** In scheme 1, prior to mixing with labeled DNA, bZIP53 and A-ZIP53 were mixed and heated to 65 °C, and cooled at room temperature. Labeled DNA was added to the protein mix and same was incubated at 25 °C for 1 h and signals were recorded. First column shows polarization signals for fluorescein labeled 5 nM 28 bps G-box containing oligo. Increased signal signifies DNA-bZIP53 complex formation after the addition of 0.5 μM bZIP53 (second column). FP signal decreased after the addition of mix of 0.5 μM bZIP53 and 1 μM A-ZIP53. **B–F)** Represent scheme 2: bZIP53 protein was added to labeled DNA and after incubation at 25 °C for 1 h, its DNA binding was challenged by the addition of two molar equivalent of A-ZIP53. FP signals were collected after incubation at 25 °C for 1 h. Unlike in EMSA, 1 μM A-ZIP53 was not heated with bZIP53 and was directly added to DNA-bZIP53 complex. Decreased signal suggests dissociated DNA from DNA-protein complex, as a result of bZIP53 interacting with A-ZIP53 (third column). Inhibition of the bZIP53 binding to the DNA by **B)** A-ZIP53, **C)** A-ZIP53(A → E), **D)** A-ZIP53(R → E), **E)** A-ZIP53(N → A), and **F)** A-ZIP53(A → E, N → A). **G)** DNA binding of bZIP53 is not affected by 1 μM A-ZIP39, a peptide that inhibit the activity of bZIP39 [30]. Results show the specificity of A-ZIP53.

decreased with increasing concentrations of A-ZIP53s. Maximum change was recorded at the equimolar concentration of bZIP53 and A-ZIP53(A → E, N → A). Differences in fluorescence polarization signals were plotted as a function of log concentrations of peptide inhibitor A-ZIP53 and its four derivatives (Fig. 5A–E). Curves were fitted according to following equation that gave half inhibitory concentration (IC<sub>50</sub>) values of five A-ZIP53s.

$$\frac{m_1 + (m_2 - m_1)}{1 + 10^{(x - \log IC_{50})}} \quad (4)$$

where m<sub>1</sub> are the reduced FP signals at highest concentrations of five A-ZIPs and m<sub>2</sub> represents FP signals in absence of peptide inhibitors A-ZIP53s. IC<sub>50</sub> values for five inhibitors are included (Fig. 5, panel A–E).

### 3.8. Time-dependent displacement of bZIP53 bound to fluorescein labeled DNA by five A-ZIP53s

FP assay was used to test the time-dependent ability of five peptide inhibitors to displace DNA bound bZIP53 at 25 °C (Fig. 6A–B). Here DNA bound bZIP53 (500 nM) was challenged by 1 μM A-ZIP53. Time-

dependent displacements of bZIP53 by five A-ZIP53s were studied to understand how different mutations affect heterodimerization rate. All experiments were performed at 25 °C and temperature was controlled by built-in Peltier system. After thorough mixing, FP signals were immediately and continuously recorded over 60 min. Fig. 6A shows decay of FP signals over time after the addition of 2 M excess of A-ZIP53. bZIP39 was used as negative control [30]. Unlike bZIP53, A-ZIP53 did not affect the DNA binding of bZIP53 demonstrating the specificity of designed A-ZIP53. Experiments under same conditions were performed with four variants of A-ZIP53 proteins. Decay curves were obtained by plotting FP signals over 60 min. Each curve was fitted according to Eq. (5)

$$C_0 \times \exp(-k \times x) \quad (5)$$

where C<sub>0</sub> is FP value at zero time, x is time in minutes, and k is the displacement constant. Displacement constant k values are given in Table 2.

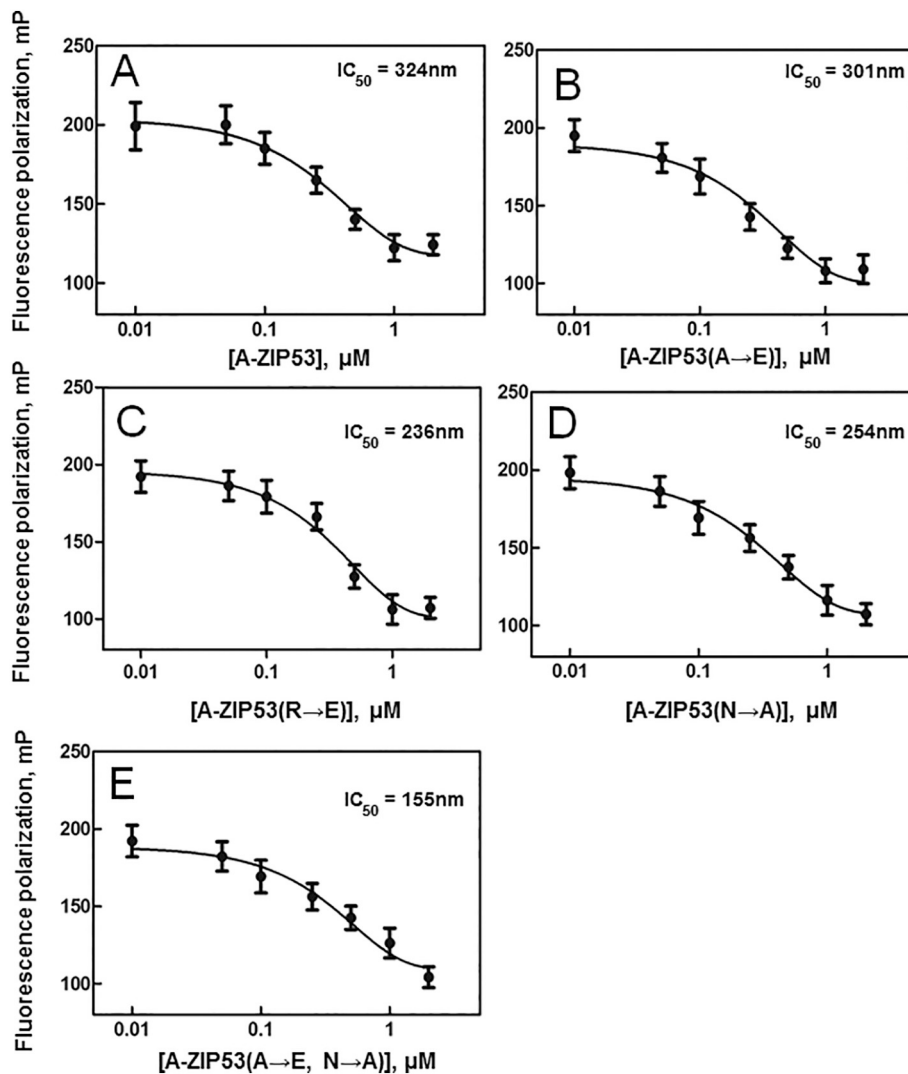


**Fig. 5.**  $IC_{50}$  values obtained for A-ZIP53s using FP assays. A) bZIP53 DNA-binding inhibition by increasing concentrations of A-ZIP53. Dose-response sigmoidal curves were fitted using eq. 4.  $IC_{50}$  for A-ZIP53 thus obtained is included in the panel A. Similarly,  $IC_{50}$  values were obtained for B) A-ZIP53(A → E), C) A-ZIP53(R → E), D) A-ZIP53(N → A), and E) A-ZIP53(A → E, N → A).

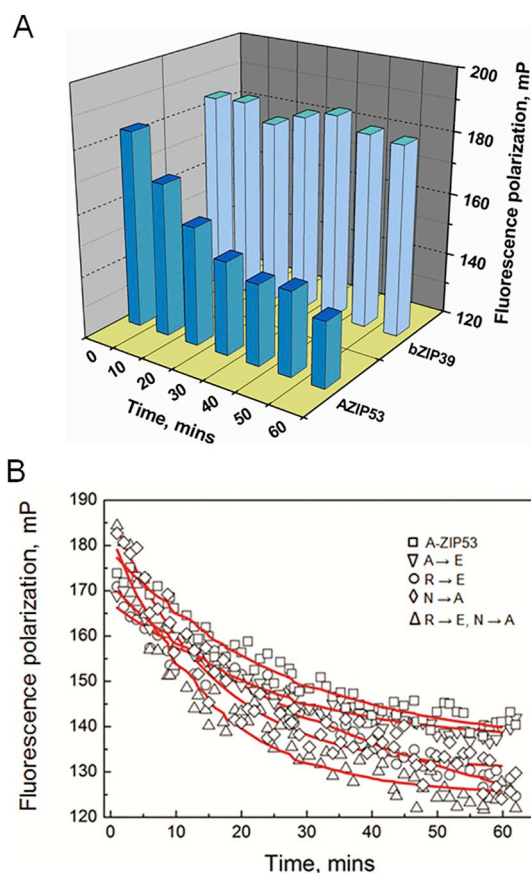
### 3.9. Transient transfection studies demonstrated the *ex vivo* activities of A-ZIP53 proteins

Fig. 7 shows the results of co-transfection experiments with bZIP53 and A-ZIP53s. *Arabidopsis* protoplasts were transfected with full length bZIP53 encoding plasmid. Translated bZIP53 protein binds to the promoter of GUS reporter gene resulting in enhanced GUS signals. NAN signals were used to normalize GUS activity. When protoplasts were co-transfected with five A-ZIP53 plasmids, bZIP53-mediated GUS signals decreased significantly. At 1:1 molar ratio of bZIP53 and A-ZIP53, GUS reporter activity decreased compared to the bZIP53 control. Unlike in *in vitro* EMSA assays, equimolar A-ZIP53 does not completely inhibit the DNA binding of bZIP53. A-ZIP53(A → E), A-ZIP53(N → A), A-ZIP53(R → E) reduced the reporter activity further. Maximum inhibition of GUS activity was observed when A-ZIP53(A → E, N → A) plasmid was used. Our transfection experiments recapitulated the observations made from *in vitro* studies. To demonstrate the specificity of A-ZIP53 against bZIP53, A-ZIP39 was used as negative control. A-ZIP39 showed no effect on the bZIP3-mediated reporter activity.

## 4. Discussion

In *Arabidopsis*, bZIP53 is involved in stress response and also

regulates seed maturation specific genes like *proline dehydrogenase*, *cruciferin*, *asparagine synthase*, *CRA*, and *hydroxysteroid dehydrogenase* [6,44]. Earlier, we used five A-ZIP53 peptides, designed to interact with bZIP53 to understand heterodimerization between bZIP53, bZIP10 and bZIP25, the three bZIP TFs involved in *Arabidopsis*'s seed maturation [30]. Present study is an attempt to quantify the interaction between bZIP53 and five A-ZIP53s, and to explore if five heterodimers are formed in biological relevant temperature and time scale. Using A-ZIP53, our previous work described the dimerization properties of bZIP53 and its ability to interact with bZIP10 and bZIP25 in the absence of DNA. A limitation of previous work is that the study did not take into account the contribution of DNA in dictating dimerization. It is well known that DNA plays a prominent role in dimerization, it may encourage dimerization even in those cases where interactions are weak and monomers do not interact spontaneously. Moreover, when a transcription factor binds to DNA, the complex is more stable than the bZIP homodimer; therefore a peptide inhibitor needs to overcome this extra stability to inhibit bZIP's DNA binding. In the previous study, we did not measure the stability of DNA-bZIP53 complex to which all the heterodimeric stabilities need to be compared to, so that an able prediction can be made regarding the *in vivo* efficacies of designed proteins. We used different assays to gain insight into the mechanism of our designed peptide to interact with the bZIP53 protein and inhibit its DNA-binding



**Fig. 6.** Five A-ZIP53s displace DNA bound bZIP53 at different rates. **A)** Time-dependent displacement of bZIP53 bound to fluorescein labeled DNA. Prior to the addition of A-ZIP53, 5 nM labeled DNA was incubated with 1  $\mu$ M bZIP53 for 1 h. Histograms representations of signal decay of labeled DNA-bZIP53 complex, after addition of 2  $\mu$ M A-ZIP53. Polarization signals were measured immediately and continuously for 60 min. **B)** 2  $\mu$ M each of A-ZIP53 and its four derivatives *i.e.*, A-ZIP53(N  $\rightarrow$  A), A-ZIP53(R  $\rightarrow$  E), A-ZIP53(A  $\rightarrow$  E), and A-ZIP53(N  $\rightarrow$  A, R  $\rightarrow$  E) were added to the DNA-bZIP53 complex and polarization signals were measured continuously for 60 min. Each curve is a mean of five independent experiments. Displacement rate constants were obtained by fitting the FP vs time traces according to equation 5 and are given in Table 2.

**Table 2**  
Time-dependent displacement of bZIP53 bound to DNA.

Protein	$k^a \times 10^{-3} \text{ min}^{-1}$
bZIP53	
bZIP53 + A-ZIP53	16 $\pm$ 3
bZIP53 + A-ZIP53 (A $\rightarrow$ E)	37 $\pm$ 4
bZIP53 + A-ZIP53 (N $\rightarrow$ A)	46 $\pm$ 4
bZIP53 + A-ZIP53 (R $\rightarrow$ E)	63 $\pm$ 6
bZIP53 + A-ZIP53 (A $\rightarrow$ E, N $\rightarrow$ A)	67 $\pm$ 5

<sup>a</sup> Displacement constants obtained for A-ZIP53s. Values are average of five independent observations and  $\pm$  represent SEs.

activity; 1) Equilibrium isothermal circular dichroic studies confirm the formation of coiled coil between peptide inhibitors and bZIP53 protein, 2) At equimolar concentrations, five A-ZIP53s inhibit the DNA-binding of bZIP53, as demonstrated by EMSA, 3) FP studies confirm the efficiency of A-ZIP53s in displacing DNA bound bZIP53, 4) Displacement constants obtained using time-dependent FP studies, reveals different rate at which five A-ZIP53s interact with bZIP53. 5) Transient transfections studies suggested that A-ZIP53 peptide inhibitors reduced the bZIP53-mediated GUS activity.

We used CD spectroscopy to assess the structural changes

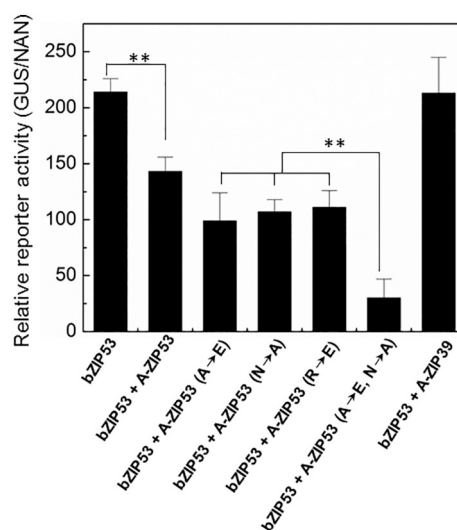


**Fig. 7.** Transient transfections show that five A-ZIP53s inhibit the bZIP53-mediated GUS gene activity. NAN gene expression was used as internal control. Reporter activity is shown as GUS/NAN. Isolated *Arabidopsis* protoplasts were transfected with various combinations of bZIP53, A-ZIP53 and A-ZIP39 expressing plasmids. bZIP53 plasmid alone enhanced the GUS reporter activity. bZIP53 transfected with A-ZIP53 demonstrated significantly reduced signals. Three variants of A-ZIP53 namely, A-ZIP53(N  $\rightarrow$  A), A-ZIP53(R  $\rightarrow$  E), and A-ZIP53(A  $\rightarrow$  E) further reduced the GUS activity. A-ZIP53(N  $\rightarrow$  A, R  $\rightarrow$  E), a plasmid carrying double mutation in acidic extension was the most effective in reducing the relative GUS activity. A-ZIP39 peptide inhibitor carrying the leucine zipper of bZIP39 did not affect the bZIP53-GUS activity demonstrating the specificity of A-ZIP53.

accompanying heterodimer formation between bZIP53 and five A-ZIP53s. All heterodimers used here showed 222/208 nm  $\geq$  1, suggesting the presence of stable coiled coil (Fig. 3E and Table 1). In the homodimer conformations, basic DNA-binding domain of bZIP53 and acidic peptide of A-ZIP53 are repulsive, resulting in low stabilities. In an equimolar mix, unstructured N-terminal regions of bZIPs and A-ZIPs form a coiled coil [38]. bZIP53 and A-ZIP53 showed 47% and 31%  $\alpha$ -helices in homodimers, whereas their equimolar mix showed 57% helices, suggesting formation of a stable heterodimer that melted with a  $T_m$  of 51.5  $^{\circ}$ C, an increase of 9.6  $^{\circ}$ C over bZIP53 (Fig. 3A and Table 1). A-ZIP53(A  $\rightarrow$  E) showed 46%  $\alpha$ -helices, a 15% gain over A-ZIP53 (Fig. 3B and Table 1). A-ZIP53(A  $\rightarrow$  E)|bZIP53 heterodimer with a  $T_m$  of 52.3  $^{\circ}$ C, showed 58%  $\alpha$ -helices (Fig. 3B and Table 1). Maximum gain in  $\alpha$ -helicity (61%) was observed for A-ZIP53(N  $\rightarrow$  A) peptide with a  $T_m$  of 53.9  $^{\circ}$ C (Fig. 3D and Table 1). Above results can be explained on the basis of  $e \leftrightarrow g'$  interactions and coupling energy of amino acids at  $a$  and  $d$  positions in a heptad upon heterodimer formation. A-ZIP53(A  $\rightarrow$  E), A-ZIP53(R  $\rightarrow$  E) are designed to introduce new  $e \leftrightarrow g'$  interactions in heterodimeric conformation with bZIP53, whereas A-ZIP53(N  $\rightarrow$  A) with the substitution of homodimer favoring asparagine at  $a$  position by an alanine, formed heterodimer with bZIP53. Our results proved our predictions and as expected A-ZIP53(A  $\rightarrow$  E, N  $\rightarrow$  A) mutant was most active in our FA and transient transfection assay. Four heterodimers involving A-ZIP53s and bZIP53 showed higher helical contents compared to individual proteins and had higher thermal stability [30]. Surprisingly, double substitution acidic extension A-ZIP53(A  $\rightarrow$  E, N  $\rightarrow$  A) with 222/208 nm = 0.83, when mixed with equimolar bZIP53 showed similar helical contents as bZIP53 homodimer but exhibited maximum stability with  $T_m$  of 55.7  $^{\circ}$ C. It is reported earlier that  $\alpha$ -helices contribute to the specificity in peptide interactions but show poor correlation with the stability parameters [31,45]. In order to design specific peptide inhibitors, the thermodynamic stability of heterodimers is paramount. Thermodynamic stability plays an important role in functionality of a protein since *in vitro* thermal stability and protein

turnover rate are negatively correlated [46,47].

We further asked the question, if A-ZIP53s can interact with DNA bound bZIP53? Five A-ZIP53s, when added to DNA-bZIP53 complex were able to displace DNA bound bZIP53 as demonstrated by decreased FA signals (Figs. 4 and 6). The results suggest that acidic peptides in A-ZIP53 offer alternative binding site for N-terminus basic region of bZIP53. nM IC<sub>50</sub> values suggest to the plausible biological applications of these inhibitors. Kinetics studies were used to discriminate between five A-ZIP53s for their abilities to interact with target bZIP53. FP decay curves showed that five A-ZIP53s were effective in displacing DNA-bound bZIP53 in biological relevant temperature and timescale, with double substitution A-ZIP53(A → E, N → A) being the most effective. We observed a good correlation between stability (T<sub>m</sub>, Table 1) and displacement constants (Table 2).

Results from *ex vivo* transient transfections co-relate well with the *in vitro* biochemical properties of the peptides. It also highlights some divergences in *in vitro* and *ex vivo* results, for example, *in vitro* EMSA studies show that all A-ZIP53s inhibit the bZIP53 DNA binding at 1:1 molar ratio whereas transfection studies could discriminate between five A-ZIPs.

After transfection, A-ZIP53 is expected to be localized in cytoplasm due to the absence of nuclear localization sequence (NLS). In a previous study, we have shown that numbers of bZIPs, with the exception of cfos, were localized in nucleus, whereas in absence of NLS, A-ZIPs were localized in cytoplasm, [48]. Co-expression of b-ZIP and A-ZIP in the cell caused the cytoplasmic localization of corresponding bZIP. A possible explanation is the formation of heterodimer between bZIP and A-ZIP heterodimer (A-ZIP|bZIP) in the cytoplasm that inactivates the NLS in the basic region of bZIP protein. This mechanism may prevent the A-ZIP|bZIP heterodimer from entering the nucleus.

A-ZIP53 inhibitor was designed to target structurally and functionally similar bZIP transcription factors *i.e.*, bZIP53, bZIP10, and bZIP25. Using A-ZIP53 as scaffold, in future, peptide inhibitors will be designed that will be specific for one bZIP TF only. For example, 5th heptad of leucine zipper region of bZIP53 has two repulsive *g↔e'* interactions (KNNVLR) [30]. It will be interesting to understand, how introducing two attractive interactions (ENNVLEA) will change its dimerization potential. We anticipate that these mutations will guide the peptide inhibitor to interact specifically with bZIP53 and not with bZIP10 and bZIP25. For biotechnology applications, A-ZIP may be used to study the role of a bZIP transcription factor *in planta* by its constitutive or tissue-specific expression in transgenic plants. Furthermore, A-ZIP inhibitors may potentially be used as switches and oscillators in system biology [49].

## 5. Conclusions

A-ZIP53 and its four derivatives were designed to preferentially heterodimerize with *Arabidopsis* bZIP53 transcription factor involved in stress response and regulation of seed maturation genes. Designed A-ZIP53s targeted the protein-protein interface of bZIP53 coiled coil and inhibited its DNA binding activity. FP equilibrium and kinetics studies demonstrated the ability of five A-ZIP53s in displacing DNA bound bZIP53. Biological activities of A-ZIP53s were shown by transient transfections studies in *Arabidopsis* protoplast system.

## Acknowledgements

We thank Executive Director, National Agri-Food Biotechnology Institute, Mohali for research facilities and Department of Biotechnology (DBT), New-Delhi for research funding. PJ acknowledges the financial assistance from DBT in the form of JRF and SRF.

## Appendix A. Supplementary data

Supplementary data to this article can be found online at <https://doi.org/10.1016/j.bbapap.2018.09.007>.

doi.org/10.1016/j.bbapap.2018.09.007.

## References

- [1] A. Barnard, K. Long, H.L. Martin, J.A. Miles, T.A. Edwards, D.C. Tomlinson, A. MacDonald, A.J. Wilson, Selective and potent proteomimetic inhibitors of intracellular protein-protein interactions, *Angew. Chem. Int. Ed. Eng.* 54 (2015) 2960–2965.
- [2] T.S. Chen, A.E. Keating, Designing specific protein-protein interactions using computation, experimental library screening, or integrated methods, *Protein Sci.* 21 (2012) 949–963.
- [3] A.W. Reinke, J. Baek, O. Ashenberg, A.E. Keating, Networks of bZIP protein-protein interactions diversified over a billion years of evolution, *Science* 340 (2013) 730–734.
- [4] A.W. Reinke, R.A. Grant, A.E. Keating, A synthetic coiled-coil interactome provides heterospecific modules for molecular engineering, *J. Am. Chem. Soc.* 132 (2010) 6025–6031.
- [5] C.R. Vinson, P.B. Sigler, S.L. McKnight, Scissors-grip model for DNA recognition by a family of leucine zipper proteins, *Science* 246 (1989) 911–916.
- [6] R. Alonso, L. Onate-Sanchez, F. Weltmeier, A. Ehlert, I. Diaz, K. Dietrich, J. Vicente-Carbajosa, W. Droge-Laser, A pivotal role of the basic leucine zipper transcription factor bZIP53 in the regulation of *Arabidopsis* seed maturation gene expression based on heterodimerization and protein complex formation, *Plant Cell* 21 (2009) 1747–1761.
- [7] M. Jakoby, B. Weisshaar, W. Droge-Laser, J. Vicente-Carbajosa, J. Tiedemann, T. Kroj, F. Parcy, Z.I.P.R.G. b, bZIP transcription factors in *Arabidopsis*, *Trends Plant Sci.* 7 (2002) 106–111.
- [8] P. Somaraj, S. Luang, S. Lopato, M. Hrmova, Basic leucine zipper (bZIP) transcription factors involved in abiotic stresses: a molecular model of a wheat bZIP factor and implications of its structure in function, *Biochim. Biophys. Acta* 1860 (2016) 46–56.
- [9] K. Dietrich, F. Weltmeier, A. Ehlert, C. Weiste, M. Stahl, K. Harter, W. Droge-Laser, Heterodimers of the *Arabidopsis* transcription factors bZIP1 and bZIP53 reprogram amino acid metabolism during low energy stress, *Plant Cell* 23 (2011) 381–395.
- [10] L. Hartmann, L. Pedrotti, C. Weiste, A. Fekete, J. Schierstaedt, J. Gottler, S. Kempa, M. Krischke, K. Dietrich, M.J. Mueller, J. Vicente-Carbajosa, J. Hanson, W. Droge-Laser, Crosstalk between two bZIP signaling pathways orchestrates salt-induced metabolic reprogramming in *Arabidopsis* roots, *Plant Cell* 27 (2015) 2244–2260.
- [11] O. Keskin, A. Gursoy, B. Ma, R. Nussinov, Principles of protein-protein interactions: what are the preferred ways for proteins to interact? *Chem. Rev.* 108 (2008) 1225–1244.
- [12] R. Rezaei Araghi, A.E. Keating, Designing helical peptide inhibitors of protein-protein interactions, *Curr. Opin. Struct. Biol.* 39 (2016) 27–38.
- [13] J.E. Darnell Jr., Transcription factors as targets for cancer therapy, *Nat. Rev. Cancer* 2 (2002) 740–749.
- [14] S. Shiozawa, K. Shimizu, K. Tanaka, K. Hino, Studies on the contribution of c-fos/AP-1 to arthritic joint destruction, *J. Clin. Invest.* 99 (1997) 1210–1216.
- [15] A. Singh, S. Venkannagari, K.H. Oh, Y.Q. Zhang, J.M. Rohde, L. Liu, S. Nimmagadda, K. Sudini, K.R. Brimacombe, S. Gajghate, J. Ma, A. Wang, X. Xu, S.A. Shahane, M. Xia, J. Woo, G.A. Mensah, Z. Wang, M. Ferrer, E. Gabrielson, Z. Li, F. Rastinejad, M. Shen, M.B. Boxer, S. Biswal, Small molecule inhibitor of NRF2 selectively intervenes therapeutic resistance in KEAP1-deficient NSCLC Tumors, *ACS Chem. Biol.* 11, (2016) 3214–3225.
- [16] P.B. Dervan, Molecular recognition of DNA by small molecules, *Bioorg. Med. Chem.* 9 (2001) 2215–2235.
- [17] B.Z. Olenyuk, G.J. Zhang, J.M. Klco, N.G. Nickols, W.G. Kaelin Jr., P.B. Dervan, Inhibition of vascular endothelial growth factor with a sequence-specific hypoxia response element antagonist, *Proc. Natl. Acad. Sci. U. S. A.* 101 (2004) 16768–16773.
- [18] V. Rishi, T. Potter, J. Laudeman, R. Reinhart, T. Silvers, M. Selby, T. Stevenson, P. Krosky, A.G. Stephen, A. Acharya, J. Moll, W.J. Oh, D. Scudiero, R.H. Shoemaker, C. Vinson, A high-throughput fluorescence-anisotropy screen that identifies small molecule inhibitors of the DNA binding of B-ZIP transcription factors, *Anal. Biochem.* 340 (2005) 259–271.
- [19] A. Eguchi, M.J. Wlekinski, M.C. Spurgat, E.A. Heiderscheid, A.S. Kropornicka, C.K. Vu, D. Bhimsaria, S.A. Swanson, R. Stewart, P. Ramanathan, T.J. Kamp, I. Slukvin, J.A. Thomson, J.R. Dutton, A.Z. Ansari, Reprogramming cell fate with a genome-scale library of artificial transcription factors, *Proc. Natl. Acad. Sci. U. S. A.* 113 (2016) E8257–E8266.
- [20] G.S. Erwin, D. Bhimsaria, A. Eguchi, A.Z. Ansari, Mapping polyamide-DNA interactions in human cells reveals a new design strategy for effective targeting of genomic sites, *Angew. Chem. Int. Ed. Eng.* 53 (2014) 10124–10128.
- [21] F. Fontaine, J. Overman, M. Moustaqil, S. Mamidyalala, A. Salim, K. Narasimhan, N. Prokoph, A.A.B. Robertson, L. Lua, K. Alexandrov, P. Koopman, R.J. Capon, E. Sierrecki, Y. Gambin, R. Jauch, M.A. Cooper, J. Zuegg, M. Francois, Small-Molecule Inhibitors of the SOX18 Transcription factor, *Cell Chem. Biol.* 24 (2017) 346–359.
- [22] S.L. Heyerdahl, J. Rozenberg, L. Jamtgaard, V. Rishi, L. Varticovski, K. Akah, D. Scudiero, R.H. Shoemaker, T.S. Karpova, R.N. Day, J.G. McNally, C. Vinson, The arylstibonic acid compound NSC13746 disrupts B-ZIP binding to DNA in living cells, *Eur. J. Cell Biol.* 89 (2010) 564–573.
- [23] X.-H. Zhang, L.Y. Tee, X.-G. Wang, Q.-S. Huang, S.-H. Yang, Off-target Effects in CRISPR/Cas9-mediated Genome Engineering, *Mol. Ther. Nucleic Acids* 4 (2015).
- [24] J. Zhao, J.R. Stagno, L. Varticovski, E. Nimako, V. Rishi, K. McKinnon, R. Akce, R.H. Shoemaker, X. Ji, C. Vinson, P6981, an arylstibonic acid, is a novel low

- nanomolar inhibitor of cAMP response element-binding protein binding to DNA, *Mol. Pharmacol.* 82 (2012) 814–823.
- [25] T. Luedde, M. Duderstadt, K.L. Streetz, F. Tacke, S. Kubicka, M.P. Manns, C. Trautwein, C/EBP beta isoforms LIP and LAP modulate progression of the cell cycle in the regenerating mouse liver, *Hepatology* 40 (2004) 356–365.
- [26] E. Magnani, N. de Klein, H.I. Nam, J.G. Kim, K. Pham, E. Fiume, M.B. Mudgett, S.Y. Rhee, A comprehensive analysis of microProteins reveals their potentially widespread mechanism of transcriptional regulation, *Plant Physiol.* 165 (2014) 149–159.
- [27] M.R. Arkin, Y. Tang, J.A. Wells, Small-molecule inhibitors of protein-protein interactions: progressing toward the reality, *Chem. Biol.* 21 (2014) 1102–1114.
- [28] M.J. Basse, S. Betzi, X. Morelli, P. Roche, 2P2Idb v2: update of a structural database dedicated to orthosteric modulation of protein-protein interactions, *Database* (2016), <https://doi.org/10.1093/database/baw007>.
- [29] A.P. Higuero, A. Schreyer, G.R. Bickerton, T.L. Blundell, W.R. Pitt, What can we learn from the evolution of protein-ligand interactions to aid the design of new therapeutics? *PLoS One* 7 (2012) e51742.
- [30] P. Jain, K. Shah, N. Sharma, R. Kaur, J. Singh, C. Vinson, V. Rishi, A-ZIP53, a dominant negative reveals the molecular mechanism of heterodimerization between bZIP53, bZIP10 and bZIP25 involved in Arabidopsis seed maturation, *Sci. Rep.* 7 (2017) 14343.
- [31] V. Rishi, J. Gal, D. Krylov, J. Fridriksson, M.S. Boysen, S. Mandrup, C. Vinson, SREBP-1 dimerization specificity maps to both the helix-loop-helix and leucine zipper domains: use of a dominant negative, *J. Biol. Chem.* 279 (2004) 11863–11874.
- [32] J. Shaikhali, J. de Dios Barajas-Lopez, K. Otvos, D. Kremnev, A.S. Garcia, V. Srivastava, G. Wingsle, L. Bako, A. Strand, The CRYPTOCHROME1-dependent response to excess light is mediated through the transcriptional activators zinc finger protein expressed in inflorescence meristem LIKE1 and ZML2 in Arabidopsis, *Plant Cell* 24 (2012) 3009–3025.
- [33] K. Arnold, F. Kiefer, J. Kopp, J.N. Battey, M. Podvinec, J.D. Westbrook, H.M. Berman, L. Bordoli, T. Schwede, The protein model portal, *J. Struct. Funct. Genom.* 10 (2009) 1–8.
- [34] F. Kiefer, K. Arnold, M. Kunzli, L. Bordoli, T. Schwede, The SWISS-MODEL repository and associated resources, *Nucleic Acids Res.* 37 (2009) D387–D392.
- [35] D. WI, PyMOL, DeLano Scientific, San Carlos, 2002 p. 700.
- [36] J. Kirby, T.A. Kavanagh, NAN fusions: a synthetic sialidase reporter gene as a sensitive and versatile partner for GUS, *Plant J.* 32 (2002) 391–400.
- [37] D. Krylov, C.R. Vinson, Leucine zipper, eLS, John Wiley & Sons, Ltd, 2001.
- [38] D. Krylov, M. Olive, C. Vinson, Extending dimerization interfaces: the bZIP basic region can form a coiled coil, *EMBO J.* 14 (1995) 5329–5337.
- [39] A. Acharya, V. Rishi, C. Vinson, Stability of 100 homo and heterotypic coiled-coil a-a' pairs for ten amino acids (A, L, I, V, N, K, S, T, E, and R), *Biochemistry* 45 (2006) 11324–11332.
- [40] A. Acharya, S.B. Ruvinov, J. Gal, J.R. Moll, C. Vinson, A heterodimerizing leucine zipper coiled coil system for examining the specificity of a position interactions: amino acids I, V, L, N, A, and K, *Biochemistry* 41 (2002) 14122–14131.
- [41] V. Rishi, P. Bhattacharya, R. Chatterjee, J. Rozenberg, J. Zhao, K. Glass, P. Fitzgerald, C. Vinson, CpG methylation of half-CRE sequences creates C/EBPalpha binding sites that activate some tissue-specific genes, *Proc. Natl. Acad. Sci. U. S. A.* 107 (2010) 20311–20316.
- [42] Y.H. Chen, J.T. Yang, K.H. Chau, Determination of the helix and beta form of proteins in aqueous solution by circular dichroism, *Biochemistry* 13 (1974) 3350–3359.
- [43] T.M. Cooper, R.W. Woody, The effect of conformation on the CD of interacting helices: a theoretical study of tropomyosin, *Biopolymers* 30 (1990) 657–676.
- [44] F. Weltmeier, A. Ehlert, C.S. Mayer, K. Dietrich, X. Wang, K. Schutze, R. Alonso, K. Harter, J. Vicente-Carbajosa, W. Droge-Laser, Combinatorial control of Arabidopsis proline dehydrogenase transcription by specific heterodimerisation of bZIP transcription factors, *EMBO J.* 25 (2006) 3133–3143.
- [45] A.J. Doig, N. Errington, T.M. Iqbalsyah, Design and Stability of  $\alpha$ -Helices, *Protein Science Encyclopedia*, Wiley-VCH Verlag GmbH & Co. KGaA, 2008.
- [46] C.L. Araya, D.M. Fowler, W. Chen, I. Muniez, J.W. Kelly, S. Fields, A fundamental protein property, thermodynamic stability, revealed solely from large-scale measurements of protein function, *Proc. Natl. Acad. Sci. U. S. A.* 109 (2012) 16858–16863.
- [47] G. McLendon, E. Radany, Is protein turnover thermodynamically controlled? *J. Biol. Chem.* 253 (1978) 6335–6337.
- [48] S.L. Heyerdahl, J. Rozenberg, L. Jamtgaard, V. Rishi, L. Varticovski, K. Akah, D. Scudiero, R.H. Shoemaker, T.S. Karpova, R.N. Day, J.G. McNally, C. Vinson, The arylstibonic acid compound NSC13746 disrupts B-ZIP binding to DNA in living cells, *Eur. J. Cell Biol.* 89 (2010) 564–573.
- [49] J.J. Tyson, R. Albert, A. Goldbeter, P. Ruoff, J. Sible, Biological switches and clocks, *J. R. Soc. Interface* 5 (2008) S1–S8.